8-2020

Modeling the Evolution of a Coupled Barrier-Marsh-Lagoon System : Insights from the New Jersey Coastline

Christopher Tenebruso
Montclair State University

Abstract:

Barriers and their associated backbarrier environments protect populated centers and infrastructure from storm impacts, support biodiversity, and provide a number of ecosystem services. Despite their socio-economic and ecological importance, the response of coupled barrier-backbarrier environments to sea-level rise is yet poorly understood. Undeveloped barrier-backbarrier systems typically respond to sea level rise through the process of landward migration, driven by storm overwash, tidal fluxes, and inland marsh upland expansion. Such response, however, can be largely affected by development and engineering activities such as dredging and shoreline stabilization techniques (e.g., seawalls, groins, beach replenishment). To better understand the difference in the response between developed and undeveloped barrier-backbarrier environments to sea-level rise, we extend a morphodynamic model that describes the evolution of a barrier-marsh-lagoon system in terms of five geomorphic boundaries: the ocean shoreline and backbarrier-marsh interface, the seaward and landward lagoon-marsh boundaries, and the upland limit of mainland marsh. We couple this numerical modeling efforts with GIS analysis and historical nautical charts that describe the evolution of Long Beach Island (LBI), New Jersey, over the last ~180 years. We find that between 1840 and 1934 the LBI system experienced landward migration of all five boundaries, including 129 meters of shoreline retreat. Despite its simplicity, the modeling framework can describe the average cross-shore evolution of the barrier-backbarrier system without accounting for human activities, suggesting that natural processes were the key drivers of morphological change during this time period. After the 1930s, however, there was a significant shift in system behavior as frequent beach nourishment, lagoon dredging, and groin construction took place during the following decades. Consequently, between 1934 and 2018 the LBI system experienced ~55 meters of shoreline progradation and a rapid decline in the area of marsh platforms. Overall, these results suggest that anthropogenic changes to overwash fluxes and estuary depths can play a major role in the evolution of barrier-backbarrier environments.

MONTCLAIR STATE UNIVERSITY

Modeling the Evolution of a Coupled Barrier-Marsh-Lagoon System: Insights from the New Jersey Coastline

by

Christopher Tenebruso

A Master's Thesis Submitted to the Faculty of

Montclair State University

In Partial Fulfillment of the Requirements

For the Degree of

Master of Science

August 2020

College of Science and Mathematics

Department of Earth and Environmental Studies

Thesis Committee:

[redacted]

Jorge Lorenzo-Trueba
Thesis Sponsor

[redacted]

Sandra Passchier
Committee Member

[redacted]

Mark Chopping
Committee Member

Modeling the Evolution of a Coupled Barrier-Marsh-Lagoon System: Insights from the New Jersey Coastline

A THESIS

Submitted in partial fulfillment of the requirements For

the degree of Master of Science

by

Christopher Tenebruso

Montclair State University

Montclair, NJ

2020

Table of Contents

1. **Introduction:**

Barrier islands front 10–13% of the world's coastlines, and this percentage is even higher in the U.S., which has the greatest length of barrier shoreline and the largest number of barriers of any country in the world (Stutz & Pilkey, 2011). These barriers and their associated backbarriers (salt marsh, lagoons, bays, tidal flats) commonly serve as buffer zones between the coastal ocean and mainland developments, including infrastructure, human population centers, and agricultural lands, and protect these investments from the impacts of storm surge and wave energy during storm events (Anarde et al., 2016; Kopp et al., 2019; Passeri, Plant, & Smith, 2015). In Figure 1, we include a map of Long Beach Island (LBI), a barrier-backbarrier environment in NJ, and a sketch of the different components in cross-section: the shoreface, continuously reworked by waves and tides, the barrier, and the backbarrier environment, which can in turn be separated into a backbarrier marsh, a lagoon, and an inland marsh. Barriers and their associated backbarrier environments also support diverse ecologic communities, and provide a wide range of ecosystem services (Barbier et al., 2011).

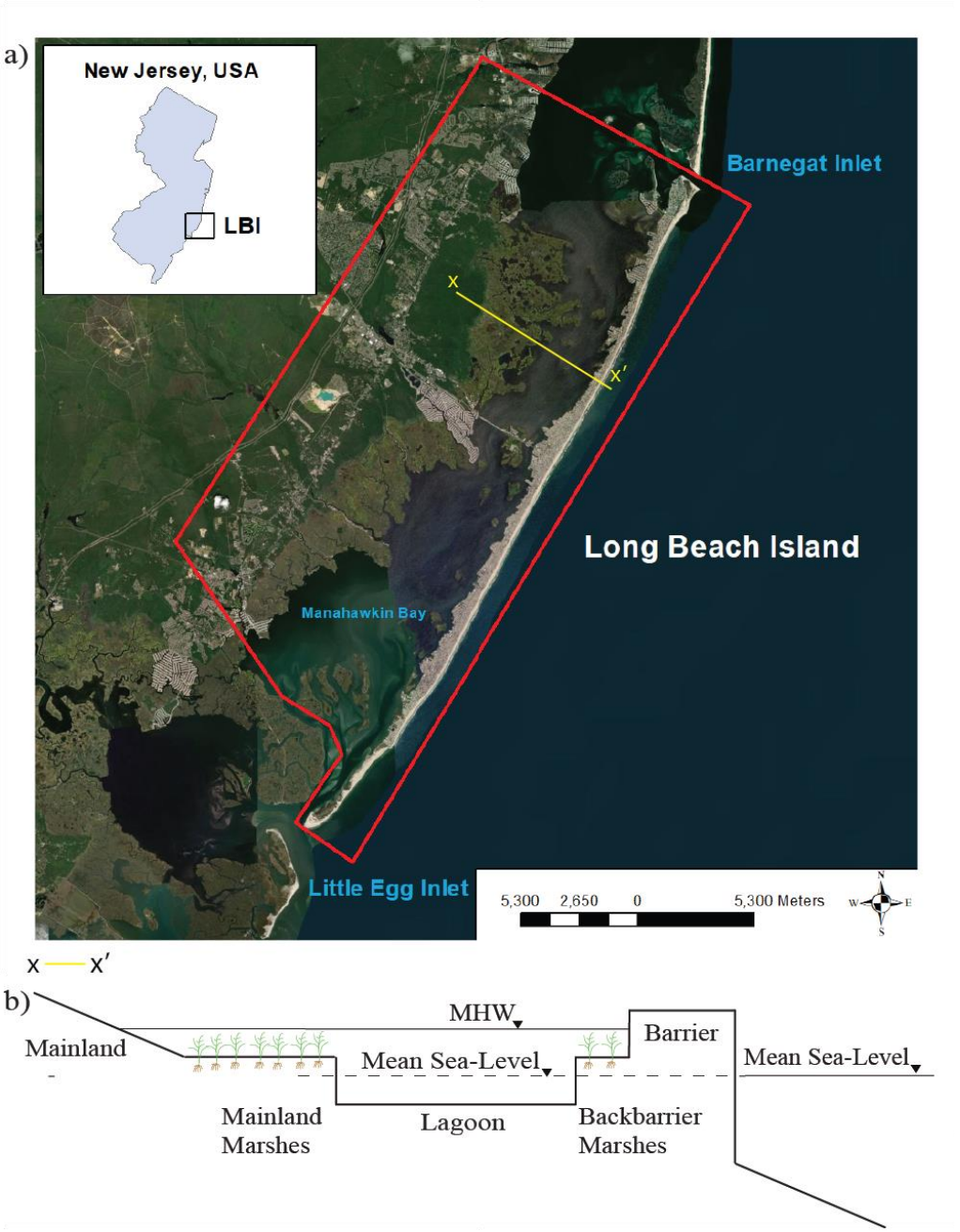

Figure 1. a) Long Beach Island New Jersey. The red polygon delimits the study site. b) The cross section x-x' is an idealized description of the barrier-backbarrier system.

Despite the economic and ecological importance of barriers, and their near ubiquity along the US East and Gulf coasts, there exists a critical gap in understanding their response to relative sea-level (RSL) rise and anthropogenic effects. Most barriers globally formed during a period of decelerating RSL rise in the middle Holocene and have migrated landward and/or stabilized and prograded since (Bruun, 1962; Church et al., 2013; FitzGerald et al., 2018; McBride et al., 2013; Pilkey, Cooper, & Lewis, 2009). Current projected CO_2-emissions scenarios predict that global rates of RSL rise will increase from ca. 1.7 mm/yr during the 20th Century to as high as ca. 8–16 mm/yr by 2100 (Church et al., 2013; Kopp et al., 2019). Such acceleration in the rate of sea level

rise can result in shoreline retreat rates significantly greater than those experienced during the 20th Century (Church et al., 2013; Mitja, Edy, & Silvia, 2018; Moore, List, Williams, & Stolper, 2010; Odezulu, Lorenzo-Trueba, Wallace, & Anderson, 2017). A rapid sea-level rise can also result in drastic changes in the backbarrier environment, including lagoon deepening and lateral expansion in detriment of marsh vegetation (Bruun, 1962; Fagherazzi et al., 2019; Kirwan, Temmerman, Skeehan, Guntenspergen, & Fagherazzi, 2016; Giulio Mariotti & Fagherazzi, 2013; Miselis & Lorenzo-Trueba, 2017; Titus & Anderson, 2009). Backbarrier geometry changes can in turn alter overwash sedimentation, enhance the tidal exchange between the ocean and the backbarrier, as well as the rate of barrier landward migration (Kirwan & Megonigal, 2013; Lorenzo-Trueba & Mariotti, 2017; Giulio Mariotti & Fagherazzi, 2013). Overall, previous field and numerical modeling efforts suggest that these two-way feedbacks between barrier islands and their associated backbarrier environments can potentially play a major role on the evolution of barrier-marsh-lagoon systems and their response to sea-level rise (FitzGerald et al., 2018; Lorenzo-Trueba & Mariotti, 2017).

To understand how barrier island systems, evolve over time we first need to define the natural processes that shape their morphology. In figure 2, we simplify the barrier system in plain view and connect both the processes that drive lateral and horizontal change. We also separate between an undeveloped and developed barrier to compare the main processes that are active in shaping their evolution. For an undeveloped barrier (figure 2a) active processes include overwash which is the movement of sediment from the shoreface to the backbarrier via storm surge (Ciarletta, Shawler, Tenebruso, Hein, & Lorenzo-Trueba, 2018; Deaton, Hein, & Kirwan, 2017; Lorenzo-Trueba & Mariotti, 2017; McBride et al., 2013; Miselis & Lorenzo-Trueba, 2017). Lateral sediment transportation which causes sediment erosion at the shoreface and when combined with overwash drives the migration of both the ocean shoreline and barrier bay shoreline. Lagoon dynamics are primarily controlled by the initial geometry of the lagoon and the abundance of suspended sediments (Kirwan et al., 2016; G Mariotti & Canestrelli, 2017; Giulio Mariotti & Fagherazzi, 2013; Nowacki & Ganju, 2019). Lagoon geometry will determine wave energy which creates marsh edge erosion and the concentration of suspended sediments will aid marsh edge growth (Kirwan & Megonigal, 2013; Kirwan et al., 2016; Leonardi, Defne, Ganju, & Fagherazzi, 2016; Giulio Mariotti & Fagherazzi, 2013; Sepanik, 2017). Although natural processes are in general the drivers of morphological change in barrier-backbarrier environments, the effect of human activities and development on these barriers has played an increasing role over past decades (Hapke, Kratzmann, & Himmelstoss, 2013; Miselis & Lorenzo-Trueba, 2017). Coastal communities have decided to "hold the line" with either soft (i.e. beach nourishment) or hard engineering structures, instead of retreating (Hapke et al., 2013). Such engineering activities can alter natural evolution of the barrier-backbarrier environment by, for instance, reducing overwash sedimentation on top and behind the barrier (Miselis & Lorenzo-Trueba, 2017; Rogers et al., 2015). Additionally, developed barrier islands are more likely to present deeper backbarrier lagoons due to dredging activities for navigation (figure 2b) (Miselis & Lorenzo-Trueba, 2017).The evolution of developed barriers is poorly understood prior to human intervention, primarily due to the lack of a quantitative understanding of the relative roles of natural processes and human activities on barrier-backbarrier system response.

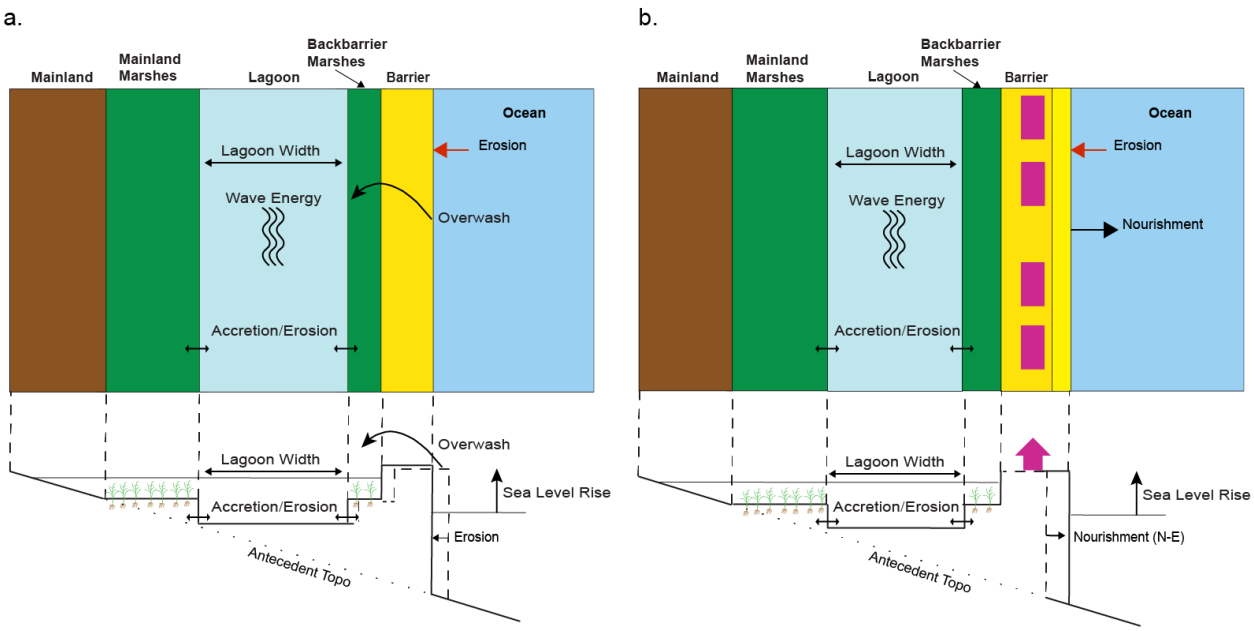

Figure 2. A plan view and cross-section illustration of an idealized undeveloped (a) and developed (b) barrier system with the active processes that drive system change.

The objective of this manuscript is to improve our quantitative understanding of the evolution of both developed and undeveloped barrier-backbarrier systems. We tackle this knowledge gap by integrating observations of LBI, extracted from historical images from 1840 to the present, and a morphodynamic model for barrier-backbarrier evolution. From field observations, LBI's past can be split into two phases that characterize its historical evolution. With the first phase occurring between 1840 and 1934, the barrier system is migrational and boundary change is unaffected by the early presence of colonial activity (Figure 3) ("LBI Chamber of Commerce," ; US Army Corps of Engineers, 1999). The second phase occurs from 1934 to 2018 where we observe a fully developed LBI system. During this time the island no longer migrates towards the mainland and system boundary direction is heavily influenced by anthropogenic forcing, creating a fixed barrier and visible reduction in marsh area. LBI's longstanding nature as a place of societal importance provides a unique opportunity to document this two phased evolution. Detailed nautical charts provide a historical record long enough to view instances where model results fall short of capturing natural process, while adjustments to model design correct flaws in interpretations of coastal dynamics that are overly reliant on pure visuals.

2. Centennial Evolution of LBI: Insights from Historical Maps

Long Beach Island New Jersey is a barrier island located on the southern half of the New Jersey coastline and is around 34km long. Its separated from the other barriers north and south by two inlets, the Barnegat Inlet (north) and the Little Egg Inlet (south). The Barnegat and Manahawkin bays separate the barrier island from the mainland. This marsh platform contains a portion of the larger Edwin B. Forsythe National Wildlife Refuge (Figure 1). Generally, the New Jersey coast can be characterized as a mixed-energy micro-tidal coastline with alongshore currents moving in a southward direction along LBI ("New Jersey Geologic History," ; Uptegrove et al., 2012; US Army Corps of Engineers, 1999). The Geology of LBI can be described as having an initial underlying layer comprised of channel and baymouth deposits dating back to the Pleistocene which

stretches from the offshore back towards the mainland (Uptegrove et al., 2012). Above layers contain bay/estuarine deposits and then barrier/shoal deposits (where the barrier is currently located) dating to the Holocene (Uptegrove et al., 2012; US Army Corps of Engineers, 1999). This sequence of layers is indicative of a transgressive barrier system where the barrier sediments are migrating up and over earlier deposits of marsh and bay sediments. Uptegrove 2012, has estimated that the LBI system has been actively transgressing since the last low stand around 18ka, and offshore relic dune/estuarine deposits can be found. This characterization of a transgressive barrier system can be observed in LBI's early evolution were the barrier boundaries are migrating towards the mainland.

Quantifying LBI's system evolution requires data from historical nautical charts or NOAA T-sheets which are source material for past morphological change and aid in constraining both phases of pre- and post-development on LBI. These charts can be accessed as scanned images in digital format at NOAA's "Historical maps and chart collection" database (https://historicalcharts.noaa.gov), and for the purpose of this work we use sheets from 1840, 1897, and 1934. These specific years are chosen due to a lack of accurate charts from the 19th century and 1934 represents a critical change from the undeveloped system to a developed one where all barrier boundaries are preserved after this point in time. Charts were georectified to align with modern aerial imagery in ArcGIS, using a combination of land-based and coordinate reference points. By outlining the individual features in each chart, we then superimposed the layers to gain an idea of the magnitude of change for each boundary through time. Polygons were created for the barrier and marshes which let us track the historical area change as well as their position. We simplified what is mainland marsh and backbarrier marsh by determining how far overwash sediments can influence marsh resilience to the backbarrier processes related to marsh edge erosion. Additionally, we also tested the sensitivity of whether marsh islands being included in our calculations for total marsh area will significantly change the rate of boundary movements (marsh islands are included in the average). We found that including the marsh islands in the averaged data better represented lagoonal and barrier dynamics for a coupled system. Once all polygons were made, we were then able to average the gain/loss along the entire stretch of the LBI barrier system to create inputs for the model. To achieve this, we converted the area from m^2 to km^2 and then divided by the length of the system (34 km). For the purpose of modeling all lengths are converted back to meters.

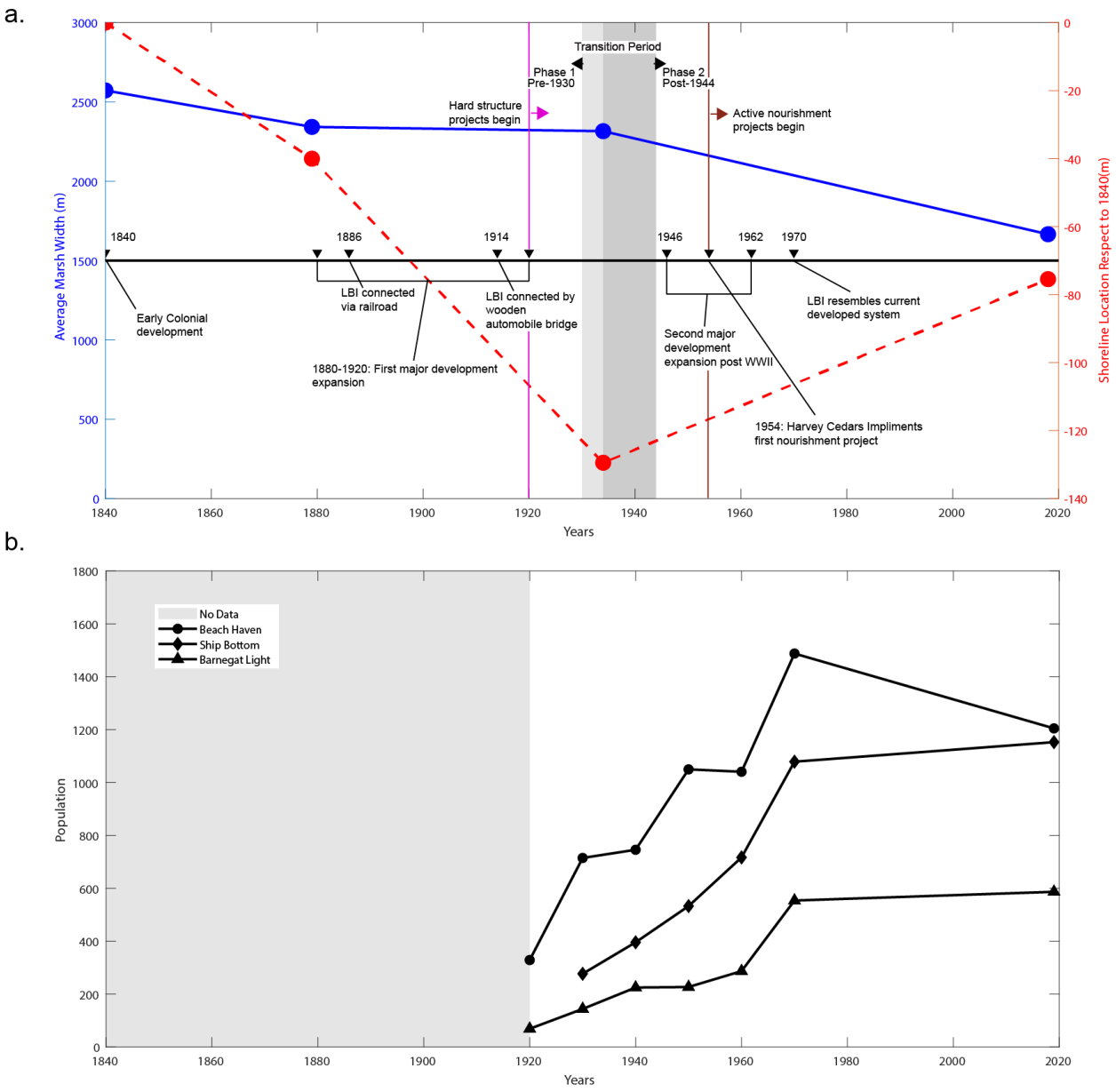

Figure 3. Tracking trends observed from GIS, (a) the timeline of human development on the barrier island system (b) tracking population data at three towns on LBI.

To justify us differentiating LBI's evolution into two phases we have accumulated supporting evidence from GIS/imagery analysis, reviewing historical records and identifying credible information from peer reviewed sources. Several aerial photographs (Figures 4, A1) are available that highlight these changes in LBI's history, providing further evidence for the rate of development seen in our imagery observations. When correlated to major events related to anthropogenic expansion we can observe the anthropogenic forcing (Figure 3). Using historical records found on the LBI chamber of commerce and the US Army Corps of Engineers websites, we reviewed these key events along with their significance to LBI's evolution through time. By doing so we gained a better insight into the separation of the two phases for its evolution. Dating back to colonial activity, semi-permanent development started to occur on LBI by the Early 1800's

(mostly for hunting and fishing) and the first manned light house was constructed in 1834. A railroad line connected LBI to the mainland in 1886 and by the early 1870's land development started to occur with the establishment of Beach Haven in 1872 and Barnegat Light in 1878. This initial development then was followed by another expansion of development that occurred between 1880 and 1920. Prior to and in 1920 increasing shoreline and inlet security became priorities for federal and local governments and initial hard structures were implemented to stabilize shorelines. Even though there seems to much development on LBI prior to the 1930's, this level of land conversion had yet to impact LBI's moving boundaries and we continue to observe shoreline retreat and bay shoreline movement into the 1930's (Figures 3 & 4). However, as we move forward in LBI's history we start to enter what we have identified as a transition between what we might still classify as an undeveloped barrier (Phase 1) to a developed barrier (Phase 2).

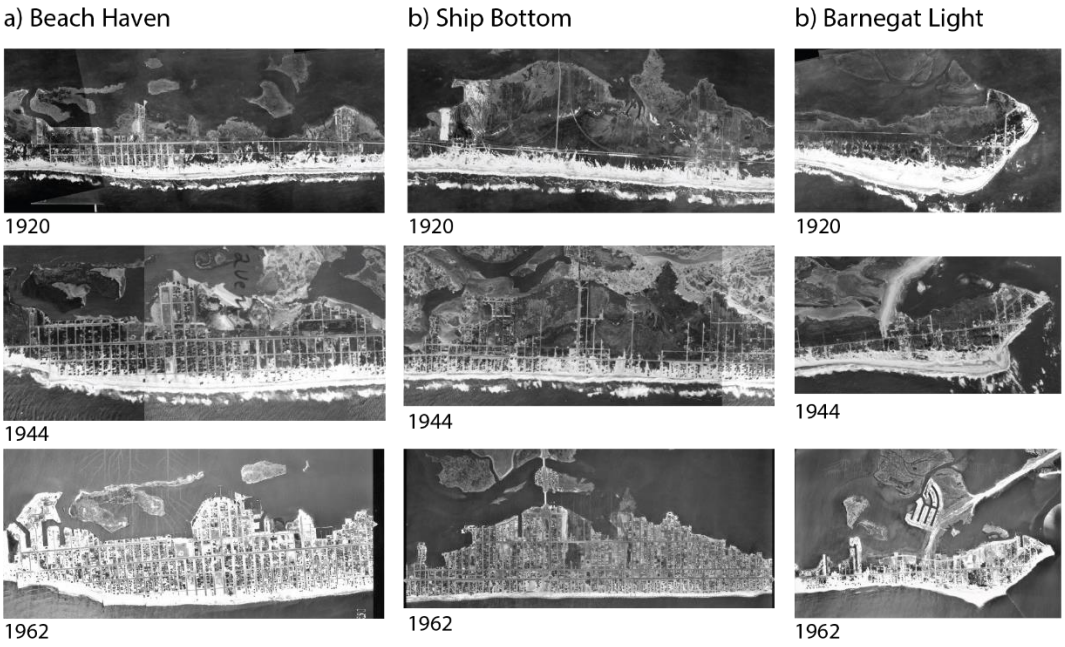

Figure 4. Imagery of several towns in LBI showing their change in land cover from 1920 to 1962.

The transition period which occured between 1934 and 1944 can be described by the increase in population on the island (Figure 3(b)); increased engineering of the coast; and the further development of empty land plots left from peacetime prior to the Second World War (Figure 4). Using census data and arial imagery, we can further describe this transition and provide supporting evidence that justifies why we chose this window of time. Using Beach Haven, Ship Bottom, and Barnegat Light as examples we can see that prior to 1930 only a few hundred people lived in these towns (Figure 3(b)). We can also see in the imagery that the barrier is sparsely developed with few structures and permanent roadways. None the less we start to see the transition occurring post 1930 as by the 1940's there is significant population increases and the initial attempts at shoreline management with the construction of wooden jetties (US Army Corps of Engineers, 1999). By the 1960's we are well into phase two with the shoreline fully engineered with sediment trapping construction and the start of nourishment projects (Trembanis, Pilkey, & Valverde, 1999; US Army Corps of Engineers, 1999; Valverde, Trembanis, & Pilkey, 1999). Notice however the geometry of the backbarrier marshes are preserved under the development

seen in the 60's which indicates that the boundary had to be fixed shortly after the 1930's to prevent the observed significant marsh loss (Figure 3(a)). After this transition period on LBI, a second land development boom occurred during 1946 to 1962 which swiftly solidifies LBI into phase 2, causing a complete shutdown in overwash by elimination of the sediments' path to the backbarrier. This rapid expansion was assisted with the start of nourishment projects in 1954 and the opening of the new four lane highway in 1956 (which replaced the railroad and the 1914 wooden bridge). By the late 1970's the island resembled its present developed state with only the redevelopment of older structures between 1980 and 2007. In addition to these historical records, the GIS has allowed the identification of several key boundary changes over time during LBI's evolution (1840 - 2018), further illustrating these two dominant phases. The first phase of LBI's evolution is summarized as on average being controlled mainly by natural processes, showing average movement towards the mainland. During the second phase, development caused barrier and backbarrier boundaries to behave counter to their natural movements. With the barrier experiencing ocean shoreline growth (and eventual fixing) and enhanced degradation of both marsh platforms. Below, we review the GIS findings in more detail and quantify the boundary movements between the two phases.

During phase I (Figure 5(a)(b)) we see an overall average area loss on all boundaries, except the backbarrier marsh, which extends its marsh-lagoon boundary due to the presence of overwash sediments. Overall, this transgressive behavior is expected for a natural barrier island system and can be compared to other barrier islands found on the East Coast. Two examples in particular can be found in Virginia: Parramore and Cedar Island are two barriers in this chain that have remained undeveloped and have been modified by similar processes found in LBI (Ciarletta et al., 2018; Sepanik, 2017). As in Virginia the barrier experiences a narrowing width due to the lack of available sediments to its shoreface. As a result, we observe the migration of the barrier boundaries towards the mainland. Post 1879 we observe normal barrier migration occurring with barrier ocean shoreline retreat coupled with its bay shoreline rolling over the backbarrier marshes (Figures 5(a), A3). As barrier migration occurs, we lose backbarrier marsh area on that boundary however, as this dynamic the marsh-lagoon edge becomes fortified with additional sediments allowing it to extend out into the lagoon. The mainland marsh-lagoon edge experiences large amounts of edge erosion and when compared to the backbarrier marshes we can observe the net benefit of an active shoreface causing barrier migration. In contrast, the mainland marsh edge is not restricted to migrate up the mainland slope due to RSL rise (Figure 5(b)).

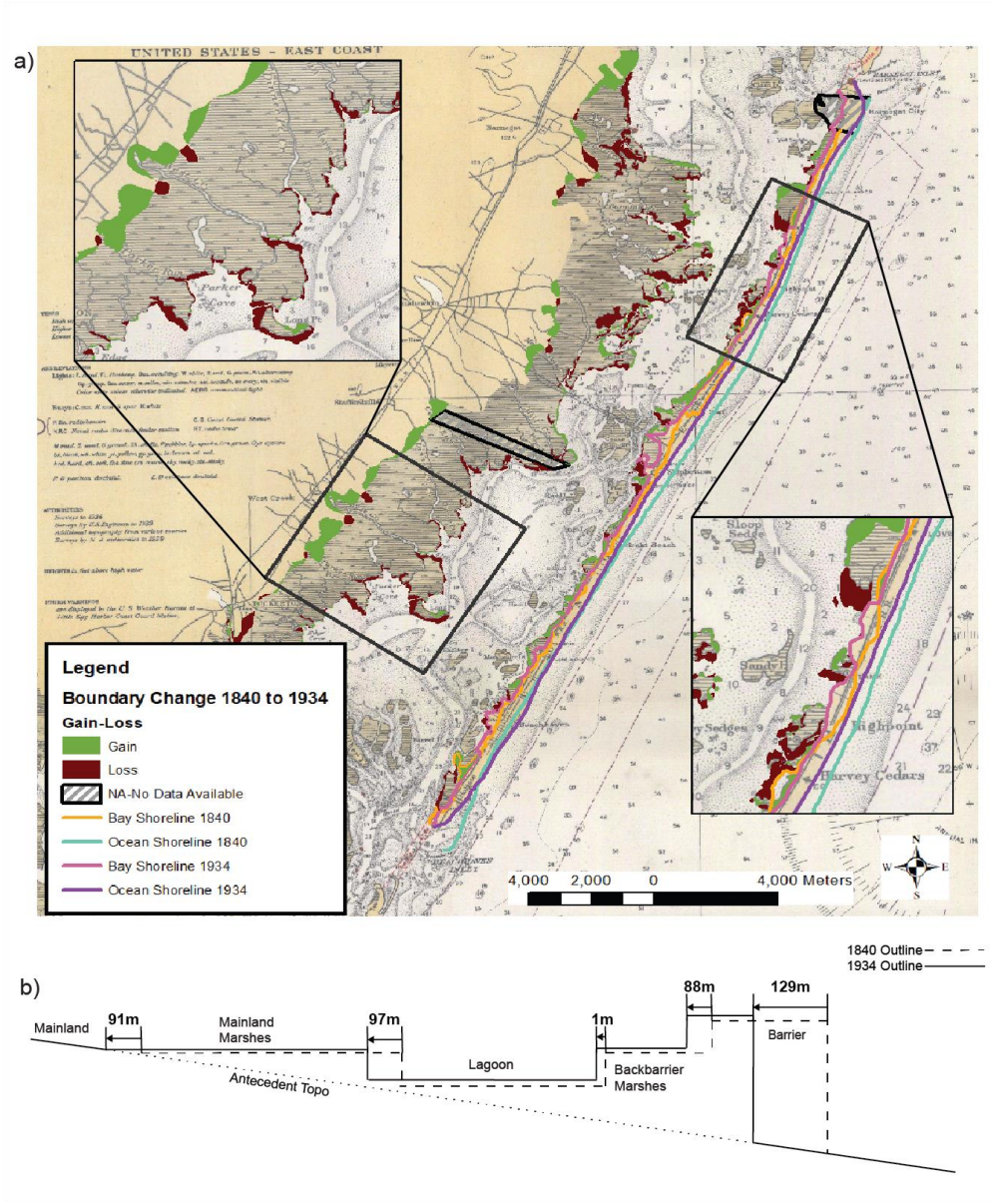

Figure 5. (a) Using historical NOAA nautical charts, we are able to compare snapshots of LBI from 1840 to 1934. During this time, we consider that the barrier island evolved without human intervention (b) the cross-section that follows the map shows average area gain or loss for each boundary and the average distance moved between time periods.

Phase two of LBI's evolution (Figure 6) is generally characterized by the rapid human development and shoreline engineering that can be observed in the above figures and imagery (Figures 3&4). During this phase, the barrier's shoreline has been modified to trap alongshore sediments (started in the 1920s) and nourishment activities started in the 1950s will cause the barrier's shoreline to grow out into the ocean. The backbarrier also becomes fixed in place and is disconnected from the processes associated with the barrier. Backbarrier marshes are almost entirely developed and what remains natural can no longer combat edge erosion from lagoon dynamics. The mainland marsh also experiences marsh-lagoon edge erosion and portions of it have also been developed. In addition, we observed a reversal in the upland migration (Figure 6b) of

the mainland marsh, most likely related to a change in subaerial topography related to mainland slope or anthropogenic forcing in the form of physical barriers to marsh upland expansion (Fagherazzi et al., 2019; Farris, Defne, & Ganju, 2019; Kirwan et al., 2016; Zinnert et al., 2019). These observations can be further reinforced by tracking the barriers shoreline position relative to total marsh area during this time (Figure 4). Once again, these behaviors are not unique to this study and can be compared to other developed islands, which include other New Jersey barriers (Hapke et al., 2013; Kirwan & Megonigal, 2013; Lazarus, Ellis, Murray, & Hall, 2016; Miselis & Lorenzo-Trueba, 2017; Rogers et al., 2015; Trembanis et al., 1999; Valverde et al., 1999). However, what is unique is our ability to constrain the timing of events and use GIS to fully quantify this transition from an undeveloped barrier system to a modern developed barrier system.

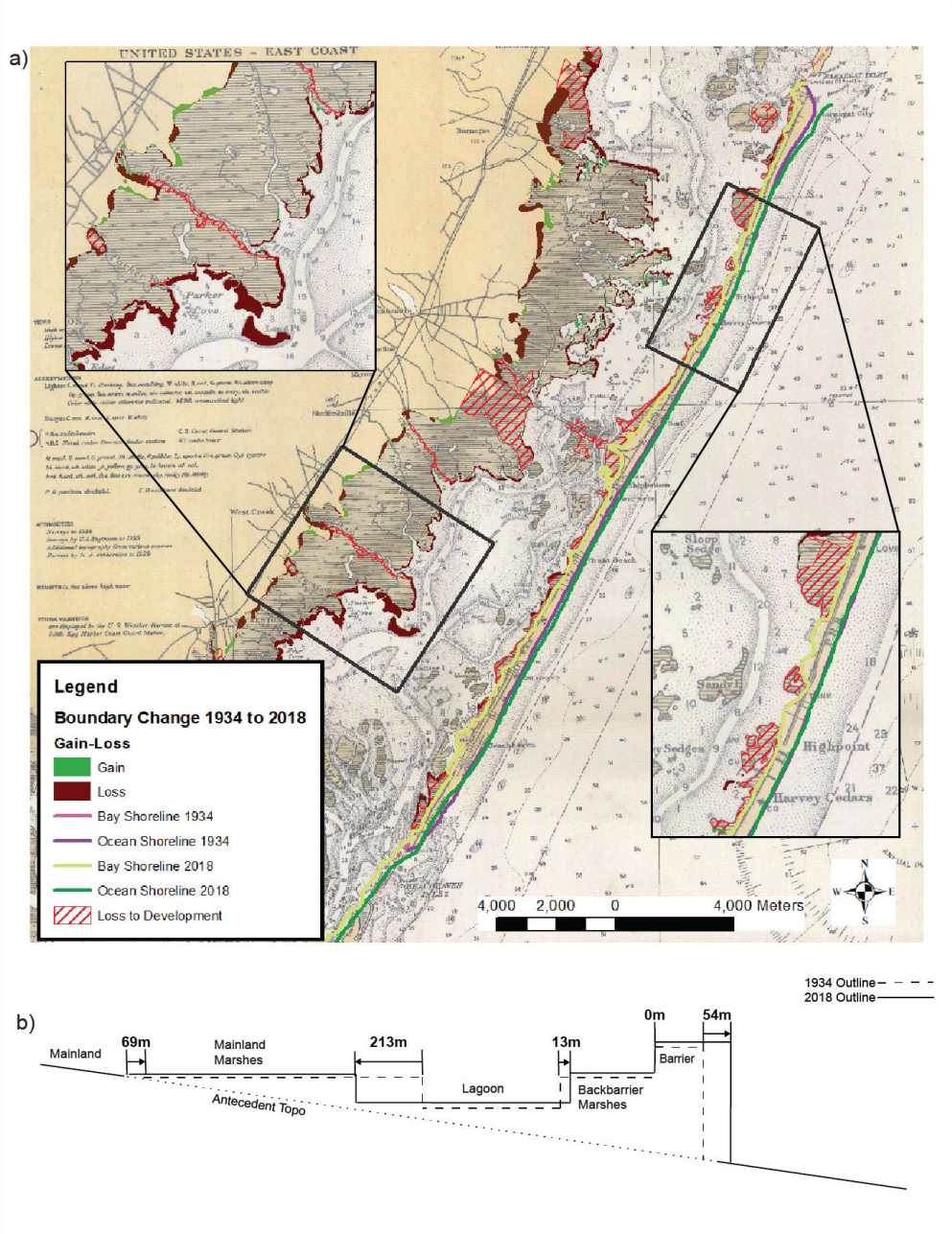

Figure 6. (a) Using historical NOAA nautical charts, we are able to compare LBI from 1934 to 2018. During this time, we consider the barrier island developed with overwash not active (b) the cross-section that follows the map shows average area gain or loss for each boundary and the average distance moved between time periods.

When we compare phase 1 (Figure 5) and phase 2 (Figure 6) there is an obvious change in barrier system evolution regarding the change in average area and direction of system boundaries. An observed disruption occurs on the barrier with the increase of development. System dynamics related to barrier migration are interrupted and instead of a retreating barrier both ocean and bay shoreline are fixed in place. With the barrier position halted, the backbarrier marsh no longer benefits from barrier migration and succumbs to lagoon erosion. Almost 40% of backbarrier marsh area was lost between 1934 and the present day, including direct marsh loss due to land conversion. This downward trend is also present with the mainland marsh where we observe a 25% loss in marsh area by 1934. This is primarily due to edge erosion and land conversion (Barbier et al., 2011; Defne et al., 2020; Farris et al., 2019; Kirwan & Megonigal, 2013; Leonardi et al., 2016; Miselis & Lorenzo-Trueba, 2017; Murray, Jenkins, Sifleet, Pendleton, & Baldera, 2010; Reeves et al., 2020). We assume that this transformation is similar to other developed barriers along the east coast. This trend in LBI can be generally summarized as during the 19th century LBI is mostly undeveloped with only temporary lodging for sport activities. It is presumed to show little to no interference with natural processes. LBI is observed being modified by processes such as overwash, sea level rise, and lagoonal dynamics, all of which drive barrier migration. We then see a transition period where rapid development and engineering occurs between the 1930's to the 1940's and a sudden shift in natural boundary behavior as seen in our data (Figure 6b). By the 1970's LBI has reached the configuration that we see in the present day and the majority of the island has been converted to urban development.

3. Numerical Modeling Framework for Barrier Evolution

Our numerical model is a modified version of a recently developed morphodynamic model (Lorenzo-Trueba & Mariotti, 2017). This modeling framework couples overwash processes, erosion, and accumulation of peat and lagoonal sediments in a dynamic framework (Figure7).

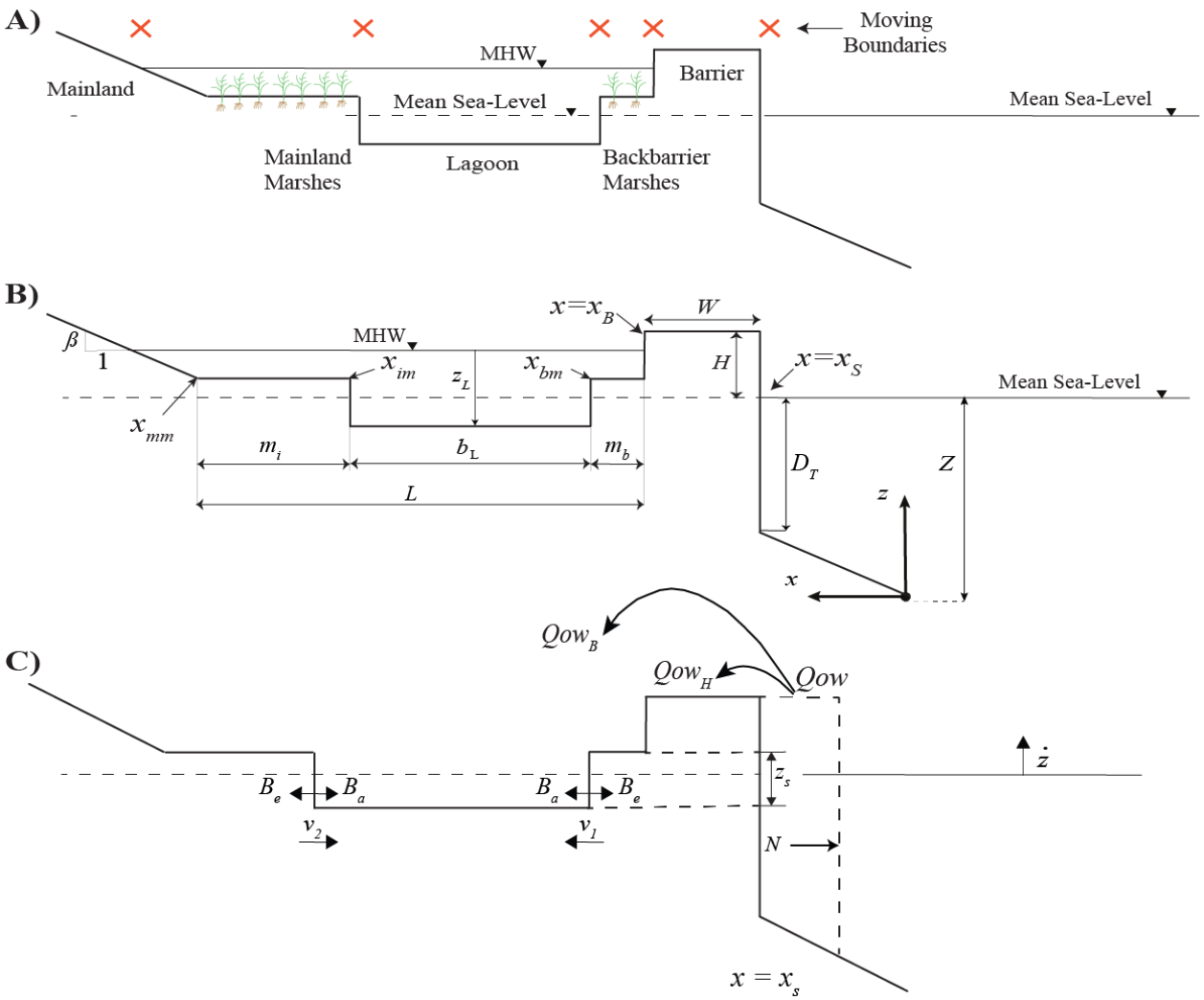

Figure 7. An idealized barrier island system composed of moving boundaries that are initialized based on real-world observations. The processes moving these boundaries are parameterized from field measurements.

Table 1. Input parameter name, symbol, and units.

Input Parameter Name	Symbol	Units
Constant Shoreface Depth	D_T	m
Elevation Relative to SLR	$\dot{z}$	m/yr
Mainland Slope	β	m/m
Nourishment rate	N	m/yr
Depth of Closure	D_T	m
Lagoon Depth	Z_L	m
Peat Thickness at the Shoreface	z_S	m

Table 2. Variable name, symbol, and units

Variable Name	Symbol	Units

Shoreface Location	x_s	m
Overwash Flux	Qow	m^2/yr
Barrier Height	H	m
Backbarrier Location	x_b	m
Backbarrier Marsh Width	m_b	m
Inland Marsh Width	m_i	m
Mainland Marsh Boundary	x_{mb}	m/m
Backbarrier System Width	L	m
Barrier Width	W	m
Rate of Migration for BMW	v_1	m/yr
Rate of Migration for MMB	v_2	m/yr
Rate of Wind-Wave Erosion	B_e	m/yr
Rate of Marsh Boundary Progradation	B_a	m/yr
Shoreface Depth	Z	m

Table 3. Initial condition name, symbol, and units

Initial Condition Name	Symbol	Units
Barrier Height	H	m
Barrier Width	W	m
Lagoon Width	b_L	m
Backbarrier Marsh Width	m_b	m
Inland Marsh Width	m_i	m
Shoreface Depth	Z	m

Two main state variables drive barrier dynamics: the ocean shoreline location x_s and the backbarrier-marsh boundary x_b. The movement of these boundaries is driven by overwash and can be determined by dividing overwash flux over the barrier's final width and height through time. Overwash flux Qow represents the movement of sediments from the shoreface to the top Qow_H, back Qow_{Bm}, and backbarrier marsh Qow_{Bl}. These sediments then support vertical barrier growth with respect to sea level rise and will move the backbarrier's shoreline location landward and provide the additional sediments to the backbarrier marsh, which provides resistance to marsh erosion. Equations 1 and 2 demonstrate how we then calculate the barrier's geometry through time utilizing overwash flux divided by the height H and shoreface depth z. Our shoreface location is further modified by subtracting our nourishment value N by a shoreface erosional value E to account for the direction of the shoreface movement, either towards (N is positive) or away (N is negative) from the ocean. The modeling framework then can separate between undeveloped and developed shorelines by simply turning off overwash and activating the nourishment value to grow out the beach, representing a developed coastline.

$$\frac{dx_s}{dt} = \frac{Qow}{H+z} - \frac{N-E}{H+z} \quad (1)$$

$$\frac{dx_b}{dt} = \frac{Qow_{Bm}}{H+z} \quad (2)$$

Another way we describe how overwash may change the rate of boundary change in the backbarrier is with the equations 3-7, where we divide the incoming overwash flux and determine where the active overwash will be added. Qow_H is the portion that is deposited to the top of the barrier and Qow_B continues to the backbarrier. There, Qow_B continues to be separated and by using ϕ as a portioning coefficient we distribute the remaining overwash flux between Qow_{Bl} (Marsh-lagoon edge) and Qow_{Bm} (Backbarrier shoreline). Where $\dot{x}_s$ is equal to $\frac{dx_s}{dt}$ and Z_s is the organic sediment thickness at the shoreface.

$$Qow_H = \dot{z} \cdot W \tag{3}$$

$$Qow_B = Qow_{Bl} + Qow_{Bm} \tag{4}$$

$$Qow_{Bl} = (1 - \emptyset)(Qow_B - \dot{x}_s \cdot Z_s) \tag{5}$$

$$Qow_{Bm} = \emptyset(Qow_B - \dot{x}_s \cdot Z_s) \tag{6}$$

$$\emptyset = min(1, \frac{bm1}{bm1c}) \tag{7}$$

Thus, the top of the marsh platforms keep pace with respect to sea level rise and at a fixed depth z_m in regard to mean high water MHW or average high tide line in the lagoon (Eq. 8). Organic accretion rate O_{ref} is the annual belowground organic matter production (Kirwan et al., 2016; Lorenzo-Trueba & Mariotti, 2017) and is calculated using the Morris et al. 2002, quadratic function of depth below mean high tide. Inorganic sediment I is then needed to satisfy the equation and occupy any remaining space.

$$\dot{z} = I + O_{ref} \tag{8}$$

Along with the vertical expansion of marsh we assume of the model is that there is a constant suspended sediment concentration in the lagoon (were sediments are re-suspended internally due to tidal fluctuations), which provides sediments to both marsh platforms in the barrier island system (equation 9). Utilizing the equation for marsh boundary progradation found in Mariotti and Fagherazzi 2013, we can calculate the accretional value being added to the marsh edges. Where w_s is the settling velocity of suspended sediments at the marsh edge, C_r is the reference sediment concentration in the lagoon, ρ is the dry sediment bulk density, and k_a is a shape factor that represents the geometry of the marsh lagoon. This allows us to simplify the lagoon dynamics, which affects marsh accretion B_a and erosion rate B_e. To calculate the marsh erosion rate, we use Eq. 10 which also is used in Marani et al. 2011 and Mariotti and Fagherazzi 2013, where k_e is the erodability coefficient, W is wave power density at the marsh platform edges, h_b is the characteristic bed level of the marsh-lagoon edge, and z_m is depth below mean high water.

$$B_a = k_a w_s C_r / \rho \tag{9}$$

$$B_e = k_e W / (h_b - z_m) \tag{10}$$

Backbarrier dynamics are primarily controlled by both marsh widths m_b (backbarrier marsh width) and m_i (mainland marsh width), which are then determined by the competition between erosional energy of the lagoon b_e and marsh edge accretion b_a. If the erosional energy can out-compete the constant growth rate of the marsh, then the marsh platforms will erode away and increase lagoon width through time. The opposite is true when the erosional energy is lower

than the accretion value, allowing the marsh platforms to grow in, narrowing the lagoon. Two additional differential equations (11 & 12) are used to describe the boundary changes through time, giving us the dimensions of the lagoon and the overall final geometry of the barrier system. Where v_1 is the rate of migration for the backbarrier marsh-lagoon edge (equation 13), v_2 is the rate of migration for the mainland marsh-lagoon edge (equation 14), $\dot{x}_b$ is equal to $\frac{dm_b}{dt}$, and β is the mainland slope.

$$\frac{dm_b}{dt} = v_1 - \dot{x}_b \tag{11}$$

$$\frac{dm_i}{dt} = v_2 + \frac{\dot{z}}{\beta} \tag{12}$$

The rates of migration for $v_1(t)$ and $v_2(t)$ are then controlled by the rate of erosion generated by the geometry of the lagoon $B_e(t)$, the rate of marsh edge accretion B_a, and the overwash flux that supplies shoreface sediments to the back barrier Qow_{Bl} divided by the length of the lagoon z_L minus the depth below mean high water z_m.

$$v_1(t) = B_a - B_e(t) + \frac{Qow_{Bl}}{z_L - z_m} \tag{13}$$

$$v_2(t) = B_a - B_e(t) \tag{14}$$

4. Results

In this section we run numerical simulations of barrier morphodynamics to investigate the roles of barrier-backbarrier interactions and human activities in the evolution of LBI over the past ~180 years. In order to conduct this analysis, we used a combination of the GIS, numerical modeling, and optimization methodology to obtain a well-rounded understanding of our results. We identified all input parameter values we use to run the model and use values either taken from field observation (GIS analysis in § 2) or scholarly review (Tables A2&A3). However not all values are constrained well and need to be optimized to fit the LBI system. We used the first phase of LBI's evolution to optimize these poorly constrained parameter values of the model and include them in tables A2, 4, and 5. Ideally, we used the sensitivity analysis in terms of regime diagrams to support the approach (Figure 8). We used a squared mean error method (Eq. 15) to provide our total error, where $n = 5$ is the number of geomorphic moving boundaries that describe the problem, with $i = 1$ to 5, and $m = 2$ are the points in time at which the error is measured, with $j = 1, 2$. We normalized the error to avoid giving more weight to some boundaries than others. Parameter values obtained by fitting to the data from phase 1 are within a physically meaningful range (Table A2). We then used the same parameter values in phase 2 with the exception of overwash and instead replace it with a nourishment value to expand out the shoreline. Utilizing this method allows us to gain insight into which parameters are more vital to the divergent behaviors seen in the field and consequently achieve the highest agreement between model and field data.

$$Error = \sum_{j=1}^{m} \sqrt{\sum_{i=1}^{n} \left(\frac{\Delta x_i}{x_i}\right)^2} \tag{15}$$

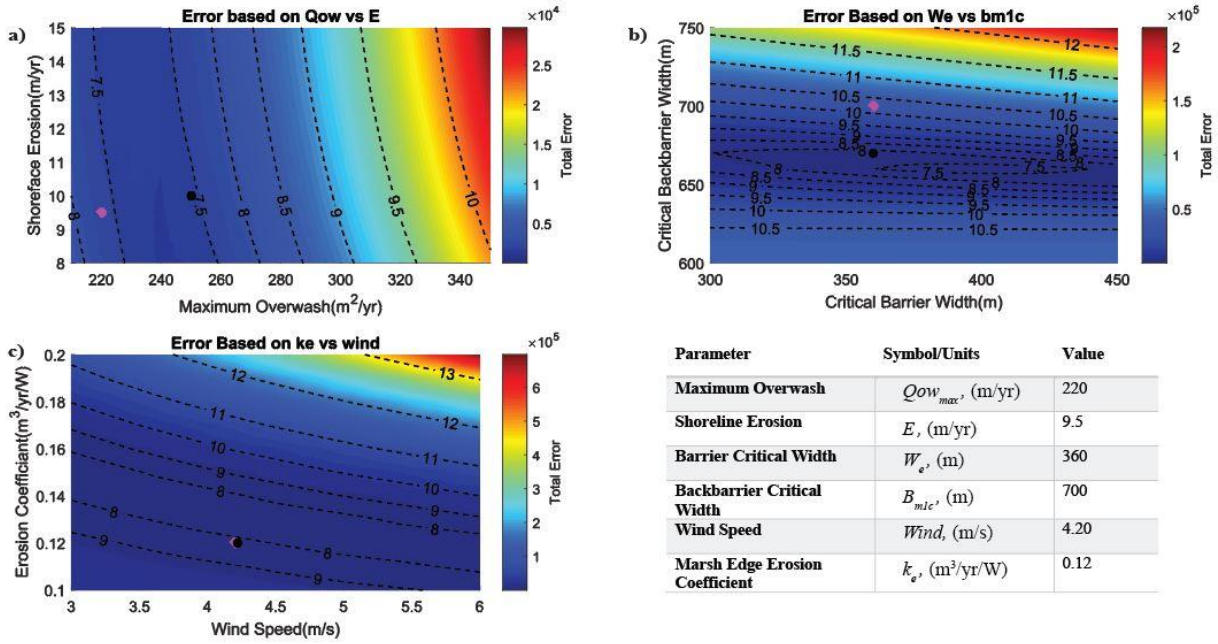

Parameter	Symbol/Units	Value
Maximum Overwash	Qow_{max}, (m/yr)	220
Shoreline Erosion	E, (m/yr)	9.5
Barrier Critical Width	W_e, (m)	360
Backbarrier Critical Width	B_{mlc}, (m)	700
Wind Speed	$Wind$, (m/s)	4.20
Marsh Edge Erosion Coefficient	k_e, (m³/yr/W)	0.12

Figure 8. Error surfaces demonstrating our model's sensitivity to parameters that are either poorly constrained or have significant control over barrier system evolution. The magenta point represents the combination of the two parameter values that yield the lowest total error for this sensitivity analysis. The black dot represents the lowest error combination for the pair yielded from the values used for the results.

Sensitivity analysis results demonstrate that the modeling framework has been fined tuned to capture barrier system dynamics in phase 1. Shown in Figure 8 we compared pairs of the optimized parameters with the addition of wind, to observe their sensitivity to a range of possible values that are physically meaningful. With all other parameters the same as shown in Table 4, the model can still acquire the lowest total error for each pair, represented by the magenta diamond. We also plot the model results in Figure 9 as black circles to compare the difference between the errors. With the addition of the wind parameter in this analysis we observe some variation in the combinations when compared to the values used in the results. However, the model still predicts a wind value close to what we identify from the field (table A2) thus reinforcing the model's ability to capture the dynamics observed on LBI. In all we find good correlation between sensitivity results and model results and are confident in our optimized parameters to describe phase 1.

To improve our quantitative understanding of barrier island response to anthropogenic forcing, we coupled the historical boundary change on LBI with the numerical model described in the previous section (Figure 7). Thus, we can compare how the model is doing with the actual movement seen historically. In general, we find agreement between model results and field observations, suggesting that barrier-backbarrier interactions play an active (and possibly dominant) role in the long-term behavior of barriers.

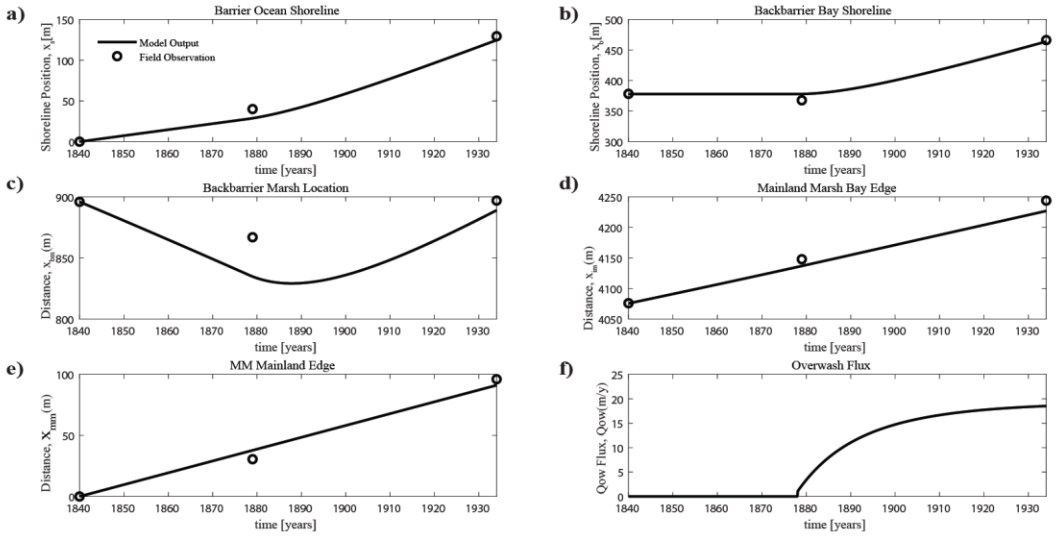

Figure 9. Model outputs for phase 1 showing a similar cross section to that seen in the field and providing data that validates the modeling framework.

Table 4. Model inputs for phase one after calibration.

Name	Symbol	Value	Units	Source
Maximum Overwash	$Qow_{,max}$	250	m^2/yr	Optimization
Mainland Slope	β	0.0032	m/m	Field Observation
Bank Erosion Coeff	k_e	0.12	m^3/yr/W	Optimization
Shoreface Erosion	E	0.70	m/yr	Optimization
Barrier Critical Width	w_e	360	m	Optimization
Backbarrier Critical Width	b_{m1c}	670	m	Optimization

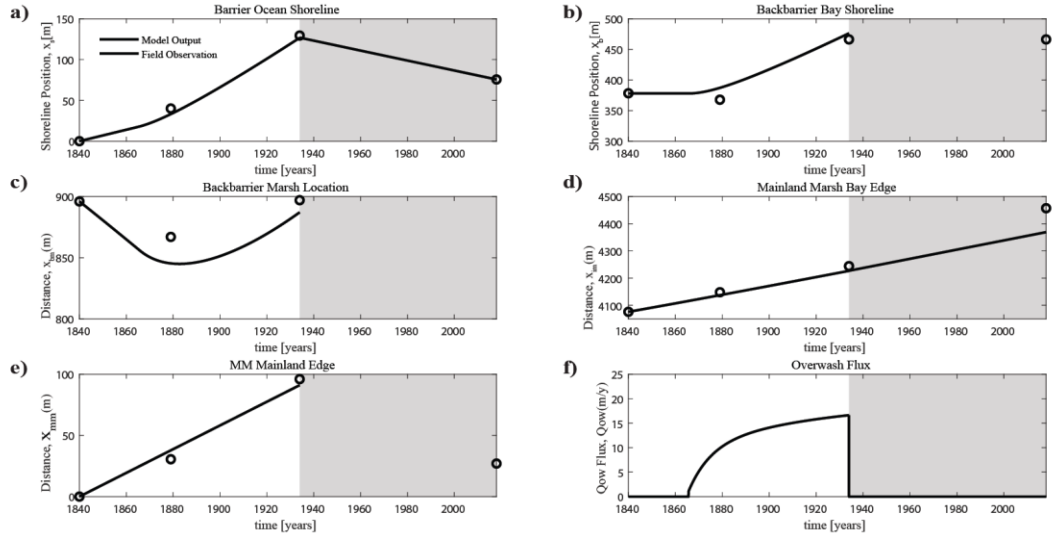

Figure 10. Phase 2 model outputs complement our field observations and demonstrate behavioral shifts in the geomorphic responses related to the tracked boundaries.

Table 5. Phase 2 model inputs after model calibration.

Name	Symbol	Value	Units	Source
Nourishment	N	1.33	m/yr	Field Observation
Mainland Slope	β	0.0032	m/m	Field Observation
Bank Erosion Coeff	k_e	0.12	m^3/yr/W	Optimization
Shoreface Erosion	E	0.70	m/yr	Optimization
Barrier Critical Width	w_e	360	m	Optimization
Backbarrier Critical Width	b_{m1c}	670	m	Optimization

The migration of the boundaries seen in LBI's phase 1 (Figure 9) is what we might expect from an undeveloped barrier island system. Subplots (a) and (b) show both the ocean shoreline and backbarrier migrating towards the mainland. This occurs due to active overwash on average moving shoreface sediments from the front of the barrier to backbarrier. It is interesting to note that the backbarrier for a brief period of time showed a movement change towards the ocean, however this behavior does not seem to play an important role in the average evolution. In subplots (c) and (d) we continue to see a trend of transgression towards the mainland where the backbarrier marshes are growing out into the lagoon due to the available overwash sediments and the mainland marsh-lagoon edge is eroding back due to the high energy lagoon. One aspect of the migrating LBI system that stands out both from our observations and modeling results is the interplay between the barrier and backbarrier marshes. Through model optimization we have constrained a site-specific critical width that best matches the LBI system. Using this value, we assume that the barrier initially was too wide for overwash sediments to make it across and deposit on the backbarrier marsh, causing the barrier to narrow through time. Once this critical barrier width is met, (seen in subplots (b), (c) and (f)) we start to see the barrier migrate again and active overwash is able to make it to the backbarrier marshes. In the particular case of LBI, backbarrier marshes are narrow enough so overwash fluxes result in backbarrier marsh expansion towards the lagoon. In some other cases, such as Deaton et al. 2017, backbarrier marshes are too wide to benefit from overwash fluxes from the ocean side. The last boundary we examine in phase 1 can been seen in subplot (e) which tracks the movement of the mainland marsh up the mainland slope. This boundary in particular is primarily controlled by the average slope and relative sea level rise rate. After calculating both we can match this trend in the modeling framework using a RSL that is acceptable for this location and the average slope needed to reproduce the inland expansion.

Model results seen in phase 2 (Figure 10) demonstrate the effect of human development on the evolution of LBI, where we observe a barrier system that has boundary movement heavily modified by anthropogenic forcing. In subplot (a) there is reversal in shoreline direction due to the restriction of overwash and the introduction of nourishment which grows out the shoreline. Due to the island's development, the backbarrier's shoreline and marshes have been fixed in place due to the lack of overwash and land conversion to residential/commercial space (seen in subplots (b) & (c)). The mainland marsh is less developed during phase two and in subplot (d) we continue to track the boundary. Although the mainland marsh-lagoon edge continues to erode and migrate towards the mainland, the model underestimates the total marsh loss for this part of LBI's evolution. We believe that a combination of anthropogenic forcing and lagoon dynamic changes are responsible for the additional erosion of the boundary; however, the modeling framework currently does not capture this response. The mainland marsh moving up the mainland slope also

experiences a reversal in migration direction and goes beyond what the current modeling framework can capture. In this case we also assume that anthropogenic forcing and topography change could be factors influencing the observed behavior.

It is necessary then to further describe the differences between the two phases in LBI's evolution and how it effects natural processes that would drive barrier evolution. More specifically we observe a breakdown of connected services that drive boundary migration through time (Figure 10). In phase one, active overwash brings sediments from the shoreface to the backbarrier thus supporting the retreat of the barrier but also aiding the health and integrity of the backbarrier marsh (Deaton et al., 2017; Theuerkauf & Rodriguez, 2017; Walters, Moore, Duran Vinent, Fagherazzi, & Mariotti, 2014). In addition, we see that the initial geometry of the lagoon determines the overall health of the mainland marsh and backbarrier marsh by determining how much erosional force is generated in the form of fetch. This dynamic is countered by the availability of suspended sediments in the lagoon (tidally suspended sediments) and the availability of overwash sediments specifically to the backbarrier marsh (Deaton et al., 2017; Kirwan et al., 2016; G Mariotti & Canestrelli, 2017; Giulio Mariotti & Fagherazzi, 2013; Theuerkauf & Rodriguez, 2017; Walters et al., 2014). Once the barrier is fully developed by phase 2 these connected dynamics start to break down. Active overwash is no longer available for barrier migration and that source of sediment to the backbarrier marsh is shut down. By decreasing sediment availability and combining this with modifying the lagoon geometry both marsh platforms experience enhanced edge erosion during this phase (Lauzon et al., 2018; Lorenzo-Trueba & Mariotti, 2017; Miselis & Lorenzo-Trueba, 2017; Theuerkauf & Rodriguez, 2017; Walters et al., 2014).

The data shown in our results were the best match that the model could reproduce given the input parameters derived from the field and our optimization. However, we also tested other variations in both observed data and modeling methods. The figures and tables found in the Appendix demonstrate the several versions of tested data and their accuracy relative to model outputs. The original method for testing field observations to model outputs relied on the position of the first point in time and the last (Figures A5, A6). The model uses these positions to best predict the model output positions to make the trend fit the field data. The plots shown in the results section rely on the same method; however, we included the mid-point in the calculation and the accuracy of the overall model trends are a closer match to what was observed in the field. Another variation tested was to see how the inclusion of marsh islands present would affect the modeling accuracy. Figures A4 and A5 in the Appendix demonstrate how having marsh islands present changes the trends we see from the modeling outputs. What we observe is that the larger average back barrier marsh area changes the critical width of the backbarrier marsh; however, this does not change the model inputs for the other parameters. When compared to the plots shown in our results, we chose the data that included the marsh islands as they better match what was observed in the field and yielded the lowest error on optimization.

5. Discussion

Model results demonstrate that changes in factors that are not typically associated with the dynamics of coastal barriers, such as the lagoon width and the rate of export/import of sediments from and to the lagoon, can lead to previously unidentified complex responses of the coupled system (Lorenzo-Trueba & Mariotti, 2017). In particular, shifts in lagoon dynamics, and/or a reduction in the supply of overwash sediments to the backbarrier, can modify barrier migration rates and even trigger enhanced marsh erosion. These complex responses become even more

significant when exploring the divergent behaviors observed in LBI's two phases. Phase 1 generally represents the behavior that would be expected for a natural transgressive barrier, where all boundaries are on average moving towards the mainland. There are however exceptions found in the data, related to the timing of overwash and its ability to reach the backbarrier marshes. Since our modeling framework couples these shoreline and backbarrier dynamics we can capture the intricate relationship between overwash sediment availability and backbarrier migration rates. Another example that we find in LBI is that the backbarrier marshes are narrow enough so overwash fluxes result in backbarrier marsh expansion towards the lagoon. In some other cases, such as Deaton et al. 2017, backbarrier marshes are too wide to benefit from overwash fluxes from the ocean side. However, another study that does capture this dynamic can be seen in Walters et al. 2014, where the GEOMBEST+ model was used to capture narrow backbarrier marshes being supported by active overwash fluxes, thereby sustaining their geometry as the barrier migrates through time. In the case of our study however, the system is not entirely natural for its duration of evolution: this dynamic is disconnected in a developed barrier island and in phase 2 we observed barrier fixing and enhanced erosion to marsh platforms.

These observations are consistent with observations from another barrier island in NJ, Island Beach (Miselis & Lorenzo-Trueba, 2017). More specifically, developed barrier islands are lower and wider, and their associated lagoons are deeper due to dredging. Our model closely matches this shoreline expansion and can track the mainland marsh-lagoon edge; however, fails to account for the increased erosional pressure generated in the lagoon. Thus, the modeling results underestimate the mainland marsh-lagoon edge loss. In addition, the model can no longer track the other boundaries as they no longer follow behavior that the current modeling framework can capture. Although future evolution is very much dependent on whether (or how long) LBI continues to maintain coastal protection strategies, the dominant processes that will continue to modify the system remain in the backbarrier. If this strategy were to change in the distant future, our assumption is that the barrier would continue to migrate towards the mainland at an increased pace compared to its historical rate due to the reduction of backbarrier marshes.

Even though GIS and modeling results demonstrate we have a good understanding of LBI's past and present, there remain several limitations to our modeling framework that need further discussion. One example of this can be found in the counterintuitive results found in Figures 6(b) and 10. In the subplots found in Figure 10 we observe in panels (b), (c), and (e) plotting results were discontinued when tracking of these boundaries entered phase 2. This is due to model limitations where in the current modeling framework we have yet to capture all of the interactions associated with a developed barrier system. More specifically, once the backbarrier bay shoreline is fixed in place it is assumed to remain in the same location post-phase 1. Consequently, by fixing the backbarrier, the backbarrier marsh has also been completely lost in the system and have also not been tracked into the next phase. Unlike the last two boundaries, the mainland marsh in phase 2 migrates back down the mainland slope. The current framework does not account for this behavior, thus not allowing us to capture it in our modeling results.

Another example of model limitations can be due to the simplicity of our modeling framework where there are processes that are not accounted for but play an important role on the dynamics of the system. Alongshore sediment transport is one such process that is not completely captured by the numerical model due to the average profile that reduces the alongshore variability into one profile. However, we do account for the average sediment loss at the shoreface caused by

this process in our modeling results. This may simplify the movement of sediment along LBI's coast, which causes the movement of sediment to redistribute itself along the shoreline. Looking at the shoreline variability map provided in the Appendix (Figure A3) we can observe an average sediment loss on the northern half of the island and an average sediment gain in the south. This suggests that LBI may have been a rotational barrier while it was undeveloped, but for the purposes of our research the average shoreline movement was migrating towards the mainland. Another process not accounted for in the model is the effect of single storm events. Although critical in the evolution of barrier islands, the temporal resolution of our field-model comparison does not allow us to explore the effects of single storm events; instead, our model assumes we are averaging the effect of storms over century timescales and that storm-driven overwash would be active unless modified by anthropogenic forcing. Despite not including single storm events in this framework, we are able to capture the average dynamics of the LBI system over decadal time scales. In the future more complex dynamics can be added to this simple modeling framework to account for the various interactions found from modeling a modern developed barrier system as well as accounting for both the sensitivity in along shore sediment exchange or increased storm intensity.

6. **Conclusions**

A primary goal and unique aspect of this project is the close integration of imagery analysis and modeling efforts. However, what this modeling framework has demonstrated is that when properly calibrated this methodology can be transferred to other undeveloped and developed barrier islands. The New Jersey coastline contains numerous other barriers that have varying degrees of human development and may have evolved in a similar fashion to LBI. Equipped with the right volume of historical data we could also decipher the feedbacks driving other barrier systems evolutions and potentially capture the pivotal moments around the transition from undeveloped to developed. In our case at LBI using a combination of ArcGIS and Matlab we were able to recreate average historical system evolution from 1840 to 2018. One highlighted behavior that we model in the LBI system is the potential importance of overwash flux to the growth of the backbarrier marsh platform. Prior to development, active overwash is causing the barrier to migrate while at the same time maintaining backbarrier marsh width. When the shoreline becomes fixed and shuts down overwash, we tend to see backbarrier marsh erosion and the barrier position becomes fixed. Our current modeling framework can capture this, and we can reproduce these behaviors with a degree of error that is minimal when compared to the observed GIS analysis (Figures 9, 10).

We then offer our coupled modeling approach to help gain insight into what the near future may hold for not only LBI but other natural and developed barriers. As a tool this numerical framework can be applied to other barrier systems to asses historical and future change. For example, if we look at LBI and consider a scenario in which it can no longer sustain current management practices, what would the next century look like? Knowing how LBI behaved historically already gives us insight and the model can capture behaviors associated with undeveloped systems quite well. Having said that a future scenario where LBI loses its shoreline engineering would most likely resemble what we have seen in phase 1. If we assume the barrier remains developed, then we could also explore how current coastal management will fair against a changing climate. However, there other scenarios this model can be tuned to account for such as

the effect of varying sea level rise, increase storm energy, and fluctuations to sediment loads in the backbarrier. Ultimately climate change presents a significant challenge to coastal engineers and managers to sustain barriers over the next 50–100 years and beyond. Not only can accelerated RSL rise and increased storminess significantly affect barrier systems, but wholesale loss of barriers would also impact the landward ecosystems they protect. Thus, remaining an important topic to continue researching and we are confident that our work may answer some important question surrounding the impacts of human development on barrier island systems.

References:

Anarde, K., Kameshwar, S., Irza, N., Lorenzo-Trueba, J., Nittrouer, J., Padgett, J., & Bedient, P. (2016). Extreme storms, sea level rise, and coastal change: implications for infrastructure reliability in the Gulf of Mexico. *AGUFM, 2016*, NH31A-1881.

Barbier, E. B., Hacker, S. D., Kennedy, C., Koch, E. W., Stier, A. C., & Silliman, B. R. (2011). The value of estuarine and coastal ecosystem services. *Ecological monographs, 81*(2), 169-193.

Bruun, P. (1962). Sea-level rise as a cause of shore erosion. *Journal of the Waterways and Harbors division, 88*(1), 117-132.

Church, J. A., Clark, P. U., Cazenave, A., Gregory, J. M., Jevrejeva, S., Levermann, A., . . . Nunn, P. D. (2013). *Sea level change*. Retrieved from

Ciarletta, D., Shawler, J., Tenebruso, C., Hein, C., & Lorenzo-Trueba, J. (2018). Reconstructing Coastal Sediment Budgets from Beach- and Foredune- Ridge Morphology: A Coupled Field and Modeling Approach. *Journal of Geophysical Research*

Deaton, C. D., Hein, C. J., & Kirwan, M. L. J. G. (2017). Barrier island migration dominates ecogeomorphic feedbacks and drives salt marsh loss along the Virginia Atlantic Coast, USA. *45*(2), 123-126.

Defne, Z., Aretxabaleta, A. L., Ganju, N. K., Kalra, T. S., Jones, D. K., & Smith, K. E. (2020). A geospatially resolved wetland vulnerability index: Synthesis of physical drivers. *PLoS One, 15*(1), e0228504.

Fagherazzi, S., Anisfeld, S. C., Blum, L. K., Long, E. V., Feagin, R. A., Fernandes, A., . . . Williams, K. (2019). Sea level rise and the dynamics of the marsh-upland boundary. *Frontiers in environmental science, 7*, 25.

Farris, A. S., Defne, Z., & Ganju, N. K. (2019). Identifying Salt Marsh Shorelines from Remotely Sensed Elevation Data and Imagery. *Remote Sensing, 11*(15), 1795.

FitzGerald, D. M., Hein, C. J., Hughes, Z., Kulp, M., Georgiou, I., & Miner, M. (2018). Runaway barrier island transgression concept: global case studies. In *Barrier dynamics and response to changing climate* (pp. 3-56): Springer.

Hapke, C. J., Kratzmann, M. G., & Himmelstoss, E. A. J. G. (2013). Geomorphic and human influence on large-scale coastal change. *199*, 160-170.

Kirwan, M. L., & Megonigal, J. P. (2013). Tidal wetland stability in the face of human impacts and sea-level rise. *Nature, 504*(7478), 53-60.

Kirwan, M. L., Temmerman, S., Skeehan, E. E., Guntenspergen, G. R., & Fagherazzi, S. J. N. C. C. (2016). Overestimation of marsh vulnerability to sea level rise. *6*(3), 253.

Kopp, R. E., Gilmore, E. A., Little, C. M., Lorenzo-Trueba, J., Ramenzoni, V. C., & Sweet, W. V. (2019). Usable science for managing the risks of sea-level rise. *Earth's Future, 7*(12), 1235-1269.

Lauzon, R., Murray, A. B., Moore, L. J., Walters, D. C., Kirwan, M. L., & Fagherazzi, S. (2018). Effects of Marsh Edge Erosion in Coupled Barrier Island-Marsh Systems and Geometric Constraints on Marsh Evolution. *Journal of Geophysical Research: Earth Surface, 123*(6), 1218-1234.

Lazarus, E. D., Ellis, M. A., Murray, A. B., & Hall, D. M. (2016). An evolving research agenda for human–coastal systems. *Geomorphology, 256*, 81-90.

LBI Chamber of Commerce. Retrieved from https://welcometolbi.com/

Leonardi, N., Defne, Z., Ganju, N. K., & Fagherazzi, S. (2016). Salt marsh erosion rates and boundary features in a shallow Bay. *Journal of Geophysical Research: Earth Surface, 121*(10), 1861-1875.

Lorenzo-Trueba, J., & Mariotti, G. J. G. (2017). Chasing boundaries and cascade effects in a coupled barrier-marsh-lagoon system. *290*, 153-163.

Mariotti, G., & Canestrelli, A. (2017). Long-term morphodynamics of muddy backbarrier basins: Fill in or empty out? *Water Resources Research, 53*(8), 7029-7054.

Mariotti, G., & Fagherazzi, S. J. P. o. t. n. A. o. S. (2013). Critical width of tidal flats triggers marsh collapse in the absence of sea-level rise. 201219600.

McBride, R. A., Anderson, J. B., Buynevich, I. V., Cleary, W. J., Fenster, M. S., FitzGerald, D. M., . . . Liu, B. (2013). Morphodynamics of barrier systems: a synthesis.

Miselis, J. L., & Lorenzo-Trueba, J. J. G. R. L. (2017). Natural and Human-Induced Variability in Barrier-Island Response to Sea Level Rise. *44*(23).

Mitja, I., Edy, K., & Silvia, F. J. A. g. (2018). fate of coastal habitats in the Venice Lagoon from the sea level rise perspective.

Moore, L. J., List, J. H., Williams, S. J., & Stolper, D. (2010). Complexities in barrier island response to sea level rise: Insights from numerical model experiments, North Carolina Outer Banks. *Journal of Geophysical Research: Earth Surface, 115*(F3).

Murray, B. C., Jenkins, W. A., Sifleet, S., Pendleton, L., & Baldera, A. J. P. b. D. N. I. f. E. P. S. D. U. (2010). Payments for blue carbon: potential for protecting threatened coastal habitats.

New Jersey Geologic History. Retrieved from https://stockton.edu/coastal-research-center/njbpn/geologic-hist.html

Nowacki, D. J., & Ganju, N. K. (2019). Simple Metrics Predict Salt-Marsh Sediment Fluxes. *Geophysical Research Letters, 46*(21), 12250-12257.

Odezulu, C., Lorenzo-Trueba, J., Wallace, D., & Anderson, J. (2017). Stratigraphic and sedimentological evidence for unprecedented shoreline migration rate during historic time: Follets Island, TX. *Barrier Island Dynamics and Response to Changing Climate. New York, NY: Springer*.

Passeri, D. L., Plant, N. G., & Smith, K. E. (2015). Understanding the Dynamic Interactions of Barrier Island Morphology and Hydrodynamic Drivers. *AGUFM, 2015*, EP23B-0955.

Pilkey, O. H., Cooper, J. A. G., & Lewis, D. A. J. J. o. C. R. (2009). Global distribution and geomorphology of fetch-limited barrier islands. 819-837.

Reeves, I. R., Moore, L. J., Goldstein, E. B., Murray, A. B., Carr, J., & Kirwan, M. L. (2020). Impacts of Seagrass Dynamics on the Coupled Long-Term Evolution of Barrier-Marsh-Bay Systems. *Journal of Geophysical Research: Biogeosciences, 125*(2), e2019JG005416.

Rogers, L. J., Moore, L. J., Goldstein, E. B., Hein, C. J., Lorenzo-Trueba, J., & Ashton, A. D. (2015). Anthropogenic controls on overwash deposition: Evidence and consequences. *Journal of Geophysical Research: Earth Surface, 120*(12), 2609-2624.

Sepanik, J. M. (2017). Salt-Marsh Loss in a Barrier-Island System: Parramore and Cedar Islands, VA, from 1957 to 2012.

Stutz, M. L., & Pilkey, O. H. J. J. o. C. R. (2011). Open-ocean barrier islands: global influence of climatic, oceanographic, and depositional settings. *27*(2), 207-222.

Theuerkauf, E. J., & Rodriguez, A. B. J. E. s. F. (2017). Placing barrier-island transgression in a blue-carbon context. *5*(7), 789-810.

Titus, J. G., & Anderson, K. E. (2009). *Coastal sensitivity to sea-level rise: A focus on the Mid-Atlantic region* (Vol. 4): Climate Change Science Program.

Trembanis, A. C., Pilkey, O. H., & Valverde, H. R. (1999). Comparison of beach nourishment along the US Atlantic, Great Lakes, Gulf of Mexico, and New England shorelines. *Coastal Management, 27*(4), 329-340.

Uptegrove, J., Waldner, J., Stanford, S., Monteverde, D., Sheridan, R., & Hall, D. (2012). Geology of the New Jersey offshore in the vicinity of Barnegat Inlet and Long Beach Island. *New Jersey Geological and Water Survey, Geologic Map Series GMS*, 12-13.

US Army Corps of Engineers, N. J. D. o. E. P. (1999). *Barnegat Inlet to Little Egg Inlet: Final Feasibility Report and Integrated Final Environmental Impact Statement* Retrieved from

Valverde, H. R., Trembanis, A. C., & Pilkey, O. H. (1999). Summary of beach nourishment episodes on the US east coast barrier islands. *Journal of Coastal Research*, 1100-1118.

Walters, D., Moore, L. J., Duran Vinent, O., Fagherazzi, S., & Mariotti, G. (2014). Interactions between barrier islands and backbarrier marshes affect island system response to sea level rise: Insights from a coupled model. *Journal of Geophysical Research: Earth Surface, 119*(9), 2013-2031.

Zinnert, J. C., Via, S. M., Nettleton, B. P., Tuley, P. A., Moore, L. J., & Stallins, J. A. (2019). Connectivity in coastal systems: Barrier island vegetation influences upland migration in a changing climate. *Global change biology, 25*(7), 2419-2430.

Appendix:

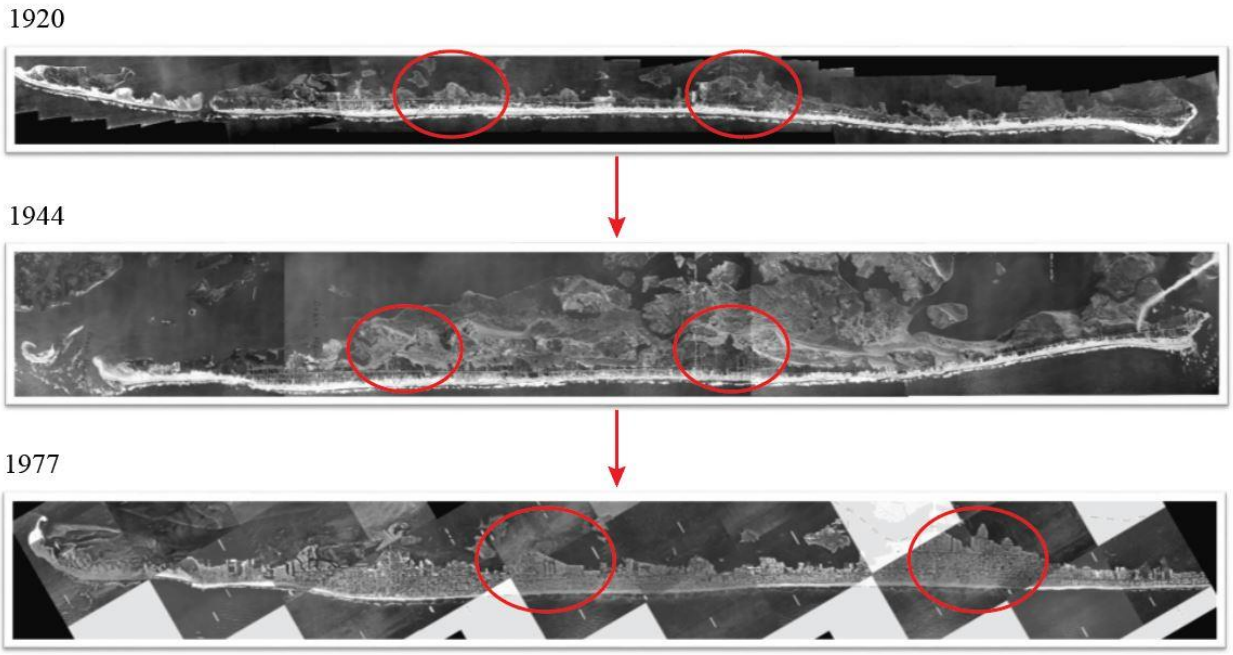

Figure A1. Analysis of LBI's historical evolution, using imagery from 1920 to 1977.

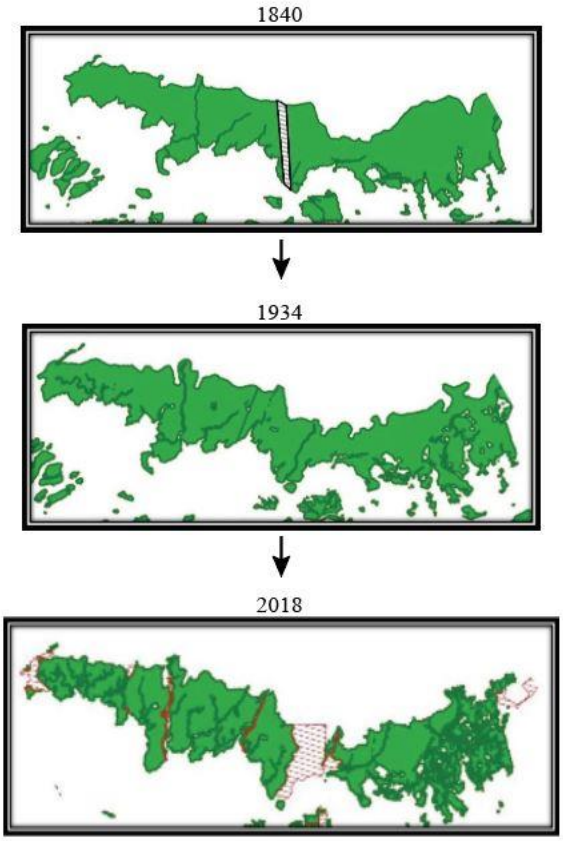

Figure A2. Analysis of LBI's mainland marsh evolution, using GIS from 1840 to 2018.

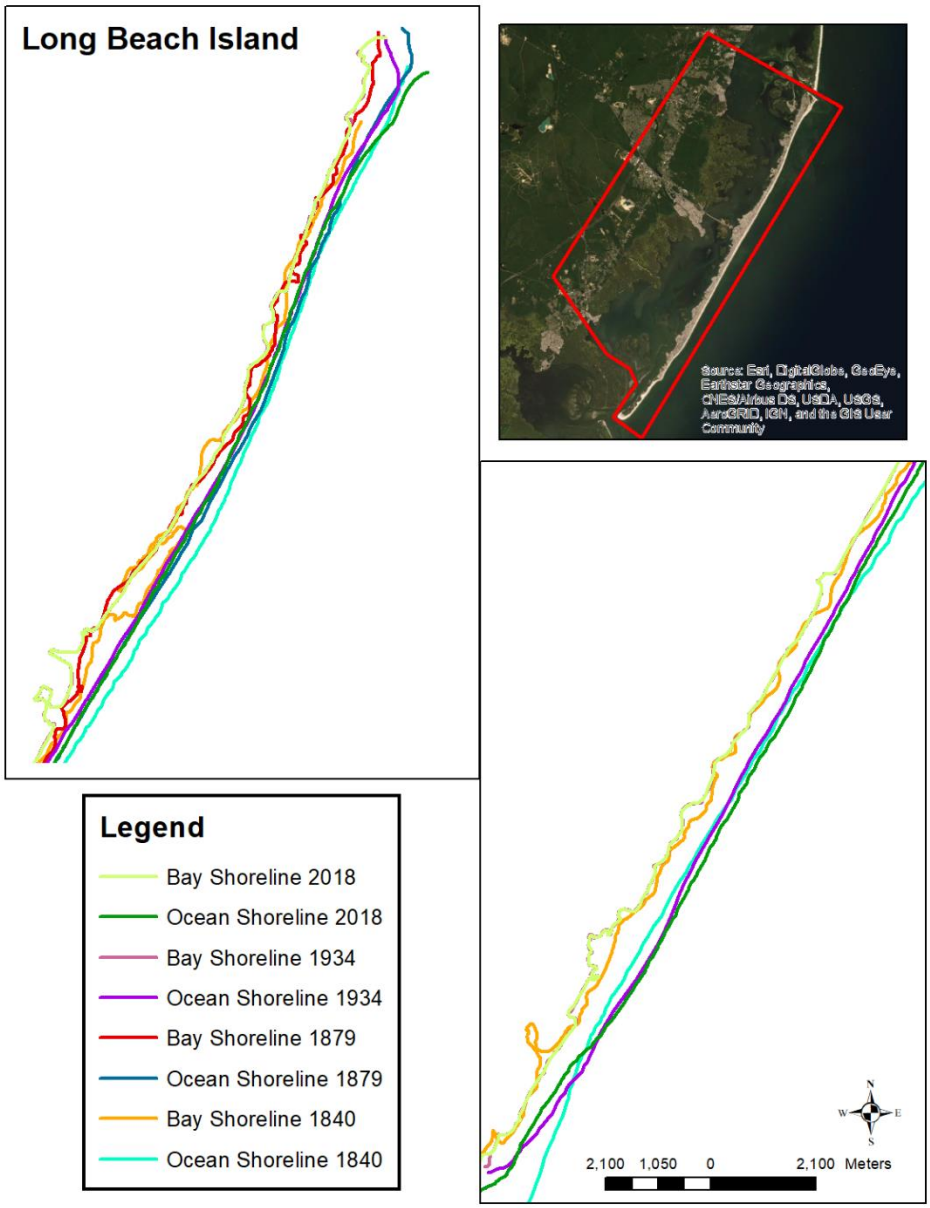

Figure A3. Shoreline variability analysis utilizing digitized nautical charts.

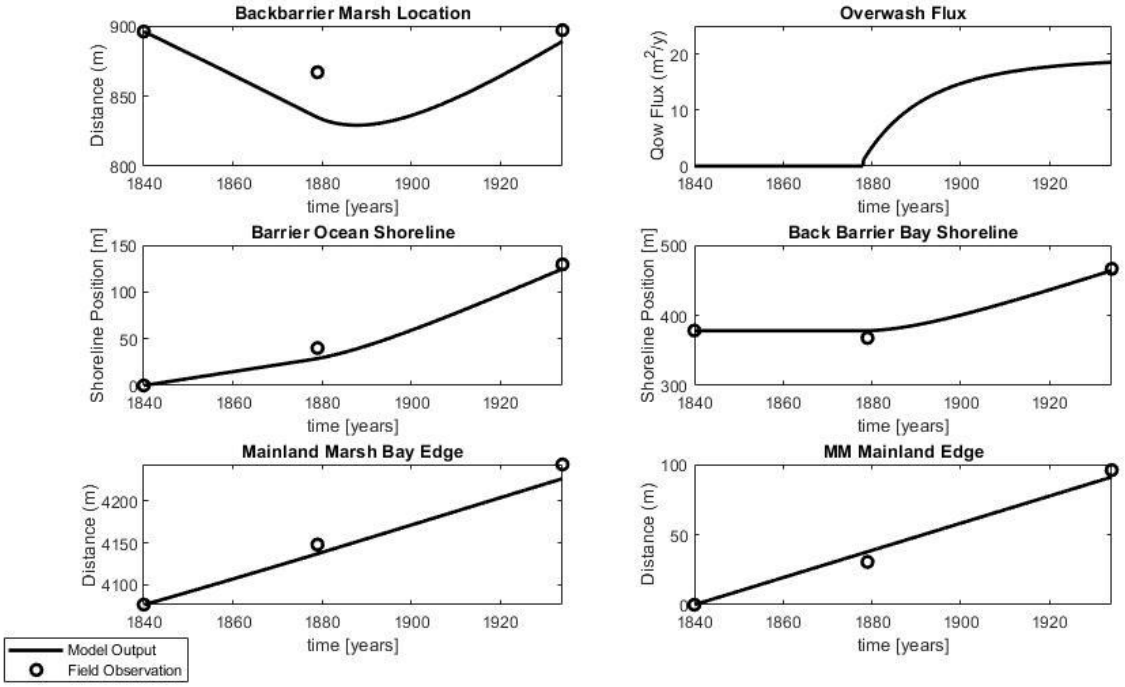

Figure A4. Data that includes marsh islands, without midpoint calculation.

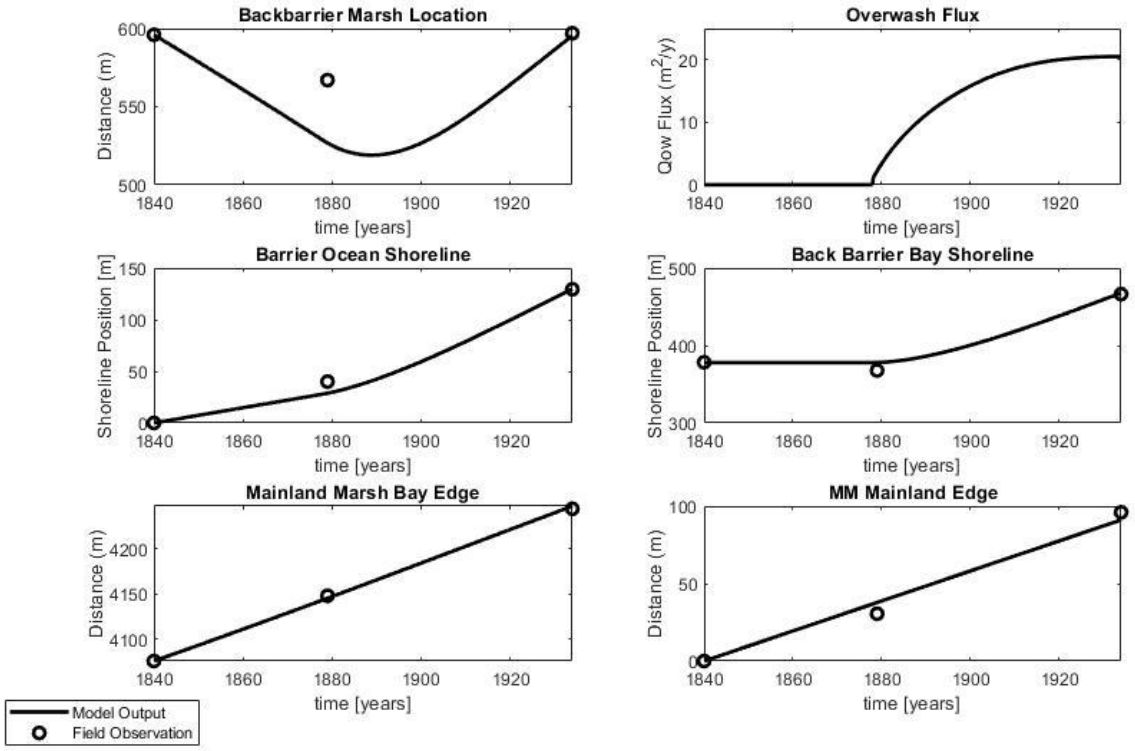

Figure A5. Data without marsh islands, includes midpoint calculations.

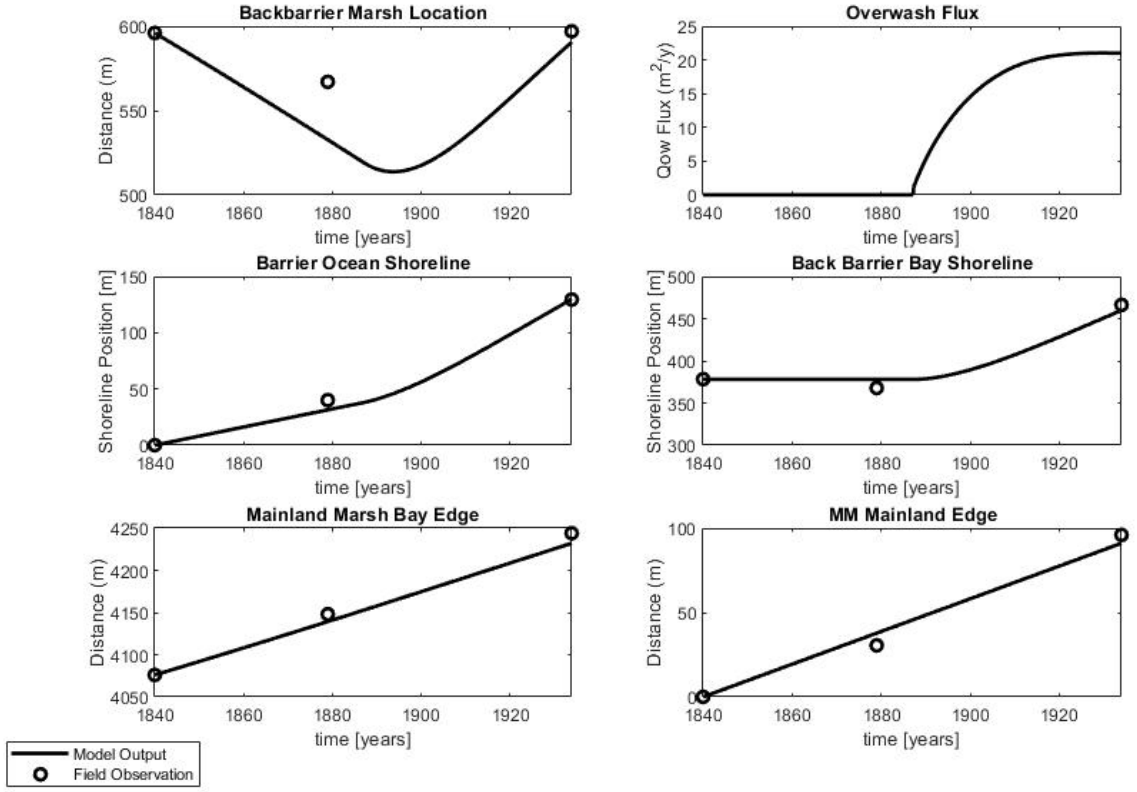

Figure A6. Data without marsh islands, includes midpoint calculation.

Table A1. Breakdown of population growth for the towns shown in Figure 4, where * represents the population at or around the date seen in the imagery.

a) Beach Haven Population	
***1920**	329
1930	715
***1940**	746
1950	1,050
***1960**	1,041
1970	1,488
Est. 2019	1,205

b) Ship Bottom Population	
***1920**	NA
1930	277
***1940**	396
1950	533
***1960**	717
1970	1,079
Est. 2019	1,153

c) Barnegat Light Population	
***1920**	69
1930	144
***1940**	225
1950	227
***1960**	287
1970	554
Est. 2019	587

Table A2. All input parameters used in our numerical framework, included is there symbol, value, value range, units, and source.

INPUT PARAMETER	SYMBOL	VALUE	VALUE RANGE (IF APPLICABLE)	UNITS	SOURCE

MAINLAND SLOPE	β	0.0032	NA	m/m	Calculated from field observations
SEA LEVEL RISE RATE	$\dot{z}$	0.0031	0.0031-0.007	m/yr	Miller et al., 2013; Miselis et al., 2017
THICKNESS OF PEAT EXPOSED AT THE SHOREFACE	z_s	0	NA	m	
MARSH DEPTH RESPECT TO MHW	z_m	0.15	NA	m	Calculated from field observations
SHOREFACE EROSION	E	10	9.5-10	m/yr	Calculated from field observations
NOURISHMENT	N	1.33	NA	m/yr	Calculated from field observations, Valverde et al., 1999; Trembanis et al., 1999
CRITICAL BARRIER WIDTH	W_e	360	NA	m	Determined by model optimization and field observation
MAXIMUM OVERWASH	Qow_{max}	250	220-250	m^2/yr	Determined by model optimization
MAXIMUM DEFICIT VOLUME	$V_{d,max}$	1,000	NA	m^2	Calculated from field observations
CONSTANT SHOREFACE DEPTH	D_T	8.22	NA	m	Calculated from field observations
ORGANIC SEDIMENT DENSITY	ρ_o	1,000	NA	kg/m^3	
POROSITY OF ORGANIC SEDIMENTS	$Porosity$	0.37	NA		
PARAMETER FOR MARSH EROSION	$dist$	10	NA	m	Calculated from field observations
TIDAL AMPLITUDE	amp	0.78	NA	m	NOAA Station: Atlantic City, NJ [8534720] Station Home
TIDAL RANGE	rng	1.56	NA	m	NOAA Station: Atlantic City, NJ [8534720] Station Home
WIND SPEED	$wind$	4.22	4.20-4.22	m/s	NOAA Station: Atlantic City, NJ [8534720] Station Home
SHAPE FACTOR THAT CAPTURES	k_a	2	NA		Mariotti and Fagherazzi 2013

THE GEOMETRY OF THE MARSH BOUNDARY					
BANK EROSION COEFFIENT	k_e	0.12	0.1-0.2	m^3/yr/W	Determined by model optimization, Mariotti and Fagherazzi 2013
MINIMUM LAGOON WIDTH	$b_{L,min}$	0	NA	m	
MAXIMUM RATE OF BIOMASS PRODUCTION	B_{max}	2.5	NA	kg/m2	Morris et al. 2002, and Table 1 in Mudd et al. 2009
CRITICAL MARSH WIDTH	b_{m1c}	670	670-700	m)	Determined by model optimization and field observation
REFERENCE CONCENTRATION IN THE LAGOON	c_r	0.001	NA	g//1=kg/m3	Mariotti and Fagherazzi 2013
ORGANIC FRACTION EXPOSED AT MARSH-LAGOON EDGE	OF_{mo}	0.5	NA		
ORGANIC SEDIMENT THICKNESS EXPOSED AT THE MARSH-LAGOON EDGE	T_{org}	0.925	NA	m	

Table A3. Shows our initial conditions for phase 1.

INITIAL CONDITION	SYMBOL	VALUE	UNITS
BARRIER HEIGHT	H	6	m
BARRIER WIDTH	W	378	m
LAGOON WIDTH	b_L	3180	m
BACKBARRIER MARSH WIDTH	m_b	518	m
INLAND MARSH WIDTH	m_i	2053	m
SHOREFACE DEPTH	D_T	8.22	m